PHILOSOPHICAL TRANSACTIONS OF THE ROYAL SOCIETY A MATHEMATICAL PHYSICAL & ENGINEERING SCIENCES

A theoretical and experimental investigation of indirectly excited roll motion in ships

I. G. Oh, A. H. Nayfeh and D. T. Mook

Phil. Trans. R. Soc. Lond. A 2000 **358**, 1853-1881
doi: 10.1098/rsta.2000.0618

THE ROYAL SOCIETY

A theoretical and experimental investigation of indirectly excited roll motion in ships

By I. G. Oh, A. H. Nayfeh and D. T. Mook

Department of Engineering Science and Mechanics, MC 0219, Virginia Polytechnic Institute and State University (VPI&SU), Blacksburg, VA 24061, USA

The phenomenon of indirectly exciting the roll motion of a vessel due to nonlinear couplings of the heave, pitch and roll modes is investigated theoretically and analytically. Two nonlinear mechanisms that cause large-amplitude rolling motions in a head or following sea are investigated. The first mechanism is internal or autoparametric resonance and the second is parametric resonance. The energy put into the pitch and heave modes by the wave excitations may be transferred into the roll mode by means of nonlinear coupling among these modes; thus, the roll can be indirectly excited. As a result, a ship in a head or following sea can spontaneously develop severe rolling motion. In the analytical approach, the method of multiple scales is used to determine a system of nonlinear first-order equations governing the modulation of the amplitudes and phases of the system. The fixed-point solutions of these equations are determined and their bifurcations are investigated. Hopf bifurcations are found in the case of two-to-one internal resonance. Numerical simulations are used to investigate the bifurcations of the ensuing limit cycles and how they produce chaos. Experiments are conducted with tanker and destroyer models. They demonstrate some of the nonlinear effects, such as the jump phenomenon, the subcritical instability, and the coexistence of multiple solutions. The experimental results are in good qualitative agreement with the results predicted theoretically.

Keywords: roll instability; internal resonance; motion coupling; saturation; experiments

1. Introduction

Around the middle of the 19th century, Froude (1863) observed that a ship whose natural frequency in pitch is twice its natural frequency in roll has undesirable seakeeping characteristics. Nearly a century later, Robb (1952) collected full-scale data on board a ship, which exhibit a continuous exchange of energy back and forth between the pitch and roll modes even though the wave motion was relatively constant. It appears that no further research on these phenomena was pursued until Kerwin (1955) used the Mathieu equation to study wave-excited roll motions. Paulling & Rosenberg (1959) then developed a set of nonlinearly coupled equations of motion to represent the motion of a vessel that was free only to pitch and roll. They neglected damping, the nonlinear effect of the roll mode on the pitch moment, and forcing terms, and derived the Mathieu equation, which they used to show that unstable roll motions

can occur for certain frequency ratios. Kinney (1961) added a linear damping term to the roll equation and essentially repeated their analysis.

Bass (1982) investigated the influence of heave-induced variations of the metacentric height, which depends on time and roll angle, on the response of a biased ship in large-amplitude beam waves. Blocki (1980) added nonlinear damping and a nonlinear restoring moment to the roll equation and used the result to investigate the probability of capsizing. Feat & Jones (1984) used a simple Duffing-type oscillator with a softening cubic nonlinearity as a model for heave-induced roll motions.

Extending Blocki's work, Sanchez & Nayfeh (1990) investigated the qualitative behaviour of rolling in head or following waves. They used an analytical–numerical technique based on the method of multiple scales to predict the qualitative changes taking place as one of the parameters is slowly changed. They confirmed their results, which included complicated responses, by using both analogue and digital computer simulations.

Kerwin (1955), Paulling & Rosenberg (1959), Kinney (1961), Bass (1982), Blocki (1980), Feat & Jones (1984) and Sanchez & Nayfeh (1990) studied the case of parametrically excited roll motions in which energy is fed to the roll mode by a prescribed pitch or heave motion, or, equivalently, head or following wave motion. However, their studies did not take into account the influence of the roll motion on the pitch and heave motions.

To explain the connection between the frequency ratio and the undesirable seakeeping characteristics, Nayfeh *et al*. (1973) used model equations that couple the pitch mode to the roll mode by including the dependence of the pitching moment on the roll orientation. Thus, the pitch (heave) motion is not prescribed but is coupled to the roll motion, and, consequently, the pitch (heave) and roll motions are determined simultaneously as functions of a prescribed excitation. They found that the pitch (heave) motion exhibits a 'saturation' phenomenon. They offered an explanation of the observation of Froude.

Nayfeh & Mook (1979) pointed out that the coupled pitch–roll problem is mathematically similar to that of describing the forced response of many elastic and dynamic systems, such as elastic pendulums, beams, arches, composite plates, and shells. All lead to systems of coupled, inhomogeneous ordinary differential equations with quadratic nonlinearities. Steady-state solutions of such systems exhibit particularly complicated behaviour when their linear undamped natural frequencies are commensurate; that is, when these systems possess internal (autoparametric) resonances. The undesirable seakeeping characteristics which Froude spoke of are manifestations of rather general behaviour that occurs in a wide variety of nonlinear physical systems. Working with structural models, Haddow *et al*. (1984), Nayfeh & Zavodney (1988) and Balachandran & Nayfeh (1991) found some of the same characteristics experimentally in structural responses. They observed the saturation phenomenon, the continuous exchange of energy back and forth between two modes coupled by an internal resonance (stable steady-state responses do not exist) when the excitation is a simple harmonic function, and chaos at larger amplitudes.

Many investigators studied the cases described above. Among them, Mook *et al*. (1974) used the method of multiple scales to analyse a simple system of two coupled oscillators with quadratic nonlinearities as a model for the coupling of pitch and roll motions. They showed that the popular approach of using Taylor-series expansions to model the hydrodynamic forces in deriving the governing equations can lead to

physically unrealistic self-sustained oscillations; they obtained more realistic equations using an energy approach. They demonstrated the existence of a saturation phenomenon when $\omega_2 \approx 2\omega_1$ and $\Omega \approx \omega_2$, where the ω_n are the linear natural frequencies and Ω is the excitation frequency. Moreover, when $\omega_2 \approx 2\omega_1$ and $\Omega \approx \omega_1$, they showed that there are conditions for which stable periodic steady-state motions do not exist. Instead, there exist amplitude- and phase-modulated motions in which the energy is continuously exchanged between the two modes. Nayfeh (1988) considered nonlinearly coupled roll and pitch motions in regular head waves in which the couplings are primarily in the hydrostatic terms when the pitch frequency is approximately twice the roll frequency and the encounter frequency is near either the pitch or the roll natural frequency. He demonstrated the saturation phenomenon when the encounter frequency is near the pitch natural frequency and demonstrated the existence of a Hopf bifurcation. He showed that initially only the pitch mode was excited, but as the wave height increased, the pitch mode saturated and energy was transferred to the roll mode. He also found a Hopf bifurcation in the response when the encounter frequency is near the roll frequency.

Next, we consider the two (parametric and autoparametric) mechanisms responsible for the roll instability, starting with the parametric mechanism.

2. Parametric excitation of roll motion

One of the mechanisms causing large-amplitude roll motions is the direct excitation of the roll mode by beam waves. The problem can be mathematically modelled by a single-degree-of-freedom roll equation having nonlinearities, constant coefficients, and an external forcing term. This mechanism of roll motion is readily understood.

Roll motion can occur even when it is not directly excited. When a vessel is in either following or head waves, violent rolling motion can occur due to parametric excitations that result from the heave–pitch–roll coupling. The excitation energy input to the pitch or heave mode may be transferred into the roll motion due to nonlinear coupling among these modes. The vessel can then exhibit a large-amplitude roll motion as well as heave and pitch motions.

Knowledge of this phenomenon is not new. Although some real experiences of rolling in head seas were reported by crews, it was believed for a long time that a vessel moving into the oncoming waves would exhibit only heave and pitch motions. In other words, a system excited by in-plane excitations will respond with in-plane modes of motion only, which is the linear result. Oh *et al.* (1992), however, found both theoretically and experimentally that this is not always true. Instead, a vessel encountering following or head waves may respond with an out-of-plane motion (roll), which can be critical to the safety of the vessel, as well as the in-plane modes of motion (heave and pitch). We summarize these results in this section.

(*a*) *Theoretical analysis*

In the traditional study of the dynamics of vessels, the response is described by a system of linear equations for small motions. By linearization, the six nonlinear coupled equations of motion are reduced to two sets of three linear equations. In this linearized model, the out-of-plane modes (yaw, sway and roll) are decoupled from the in-plane modes (pitch, heave and surge). This approach, therefore, neglects

the sometimes pronounced effects of nonlinear coupling. These coupling effects often take the form of a parametric resonance, which can lead to a particularly dangerous situation.

The possibility of large-amplitude roll motions and even capsizing due to the nonlinear interactions among the modes, which necessarily requires a multi-degree-of-freedom nonlinear formulation, began to be recognized with Froude's observation. Froude observed undesirable rolling motions due to the coupling effects between the heave and roll modes in the middle of the 19th century. However, research on nonlinear interactions between the modes was not pursued until the middle of the 20th century.

Paulling & Rosenberg (1959) attempted to address the indirect excitation of the roll mode due to energy transfer from either of the directly excited heave or pitch modes. They linearized the roll equation (it contains a time-varying coefficient) by assuming harmonic pitch and heave motions and then used the resulting Mathieu (or Hill) equation to determine conditions for the stability of trivial solutions (no-roll motions). With this approach, however, the predicted roll angle grows exponentially with time, which is unrealistic.

Kerwin (1955), Kinney (1961), Blocki (1980), Bass (1982), Feat & Jones (1984) and Sanchez & Nayfeh (1990) followed a reasoning similar to that of Paulling & Rosenberg (1959) and derived linear and nonlinear Mathieu equations. They included linear and/or nonlinear damping terms and nonlinear restoring moments in the Mathieu-equation-based roll equation and studied the case of parametrically excited roll motions, in which energy is fed to the roll mode by the prescribed pitch or heave motion, or, equivalently, wave motion.

Blocki (1980), among others, considered a ship with only two degrees of freedom (heave and roll). Such a restriction (the elimination of pitch) implies that the ship is symmetric with respect to the midship section (sometimes called fore-and-aft symmetry) and in a beam wave. Attempting to satisfy such limitations, Blocki (1980) used a simple model of a half cylinder in a beam wave in his experiments. In his analysis, he ignored the wave-induced roll moment, an obvious inconsistency but a reasonable approximation when the slope of the waves is small and the wavelength is large compared with the beam of the model. He attempted to address the parametrically excited roll motion in the presence of only the heave by assuming that pitch does not occur ($\theta \approx 0$).

Oh *et al*. (1992) improved on the previous theoretical work. They described the real situation more accurately than Blocki (1980) or Sanchez & Nayfeh (1990). Specifically, they lifted the restriction of fore-and-aft symmetry, added a third degree of freedom (pitch), and considered head and following waves both theoretically and experimentally. The heave and pitch motions were assumed to be independent of the roll motion, an assumption that was verified experimentally. These motions were considered simultaneously and assumed to be harmonic. Due to the heave–pitch–roll coupling, the amplitudes and frequencies of the heave and pitch motions play the roles of an effective amplitude and frequency of the parametric excitation. The parametric term in the roll equation accounts for the time-dependent variation of the metacentric height. They investigated the principal parametric resonance case, in which the wave frequency is approximately twice the natural frequency in roll.

We consider a model supported with three degrees of freedom: roll (ϕ), pitch (θ) and heave (z). A model set of equations of motion can be written in the following

form (Lewis 1989):

$$\ddot{z} + 2\zeta_z \dot{z} + \omega_z^2 z = Z(t), \tag{2.1}$$

$$\ddot{\theta} + 2\zeta_\theta \dot{\theta} + \omega_\theta^2 \theta = \Theta(t), \tag{2.2}$$

$$\ddot{\phi} + \omega_\phi^2 \phi + 2\mu_1 \dot{\phi} + 2\mu_3 \dot{\phi}^3 - \alpha_3 \phi^3 - \tfrac{1}{2}(K_{\phi z}\phi z + K_{\phi\theta}\phi\theta + K_{\dot{\phi}\dot{z}}\dot{\phi}\dot{z} + K_{\dot{\phi}\dot{\theta}}\dot{\phi}\dot{\theta}) = K(t), \tag{2.3}$$

where ζ_z and ζ_θ are damping coefficients; ω_z, ω_θ and ω_ϕ are the natural frequencies; μ_1 and μ_3 are linear and cubic roll damping coefficients; α_3 is the constant cubic 'stiffness' coefficient; $K_{\phi z}$, $K_{\phi\theta}$, $K_{\dot{\phi}\dot{z}}$ and $K_{\dot{\phi}\dot{\theta}}$ are the constant coefficients of the quadratic coupling terms; and Z, Θ and K are the wave excitations. Blocki (1980) ignored the kinematic–kinematic coupling and considered only heave and roll; thus, he had only one (static–static) quadratic term: $K_{\theta z}\phi z$. Here, we include additional static–static coupling as well as kinematic–kinematic coupling terms.

Assuming a simple harmonic wave excitation, we write

$$\bar{Z}(t) = \bar{Z}_0 \cos \Omega t, \tag{2.4}$$

$$\bar{\Theta}(t) = \bar{\Theta}_0 \cos(\Omega t + \tau_\sigma), \tag{2.5}$$

where Ω is the frequency of the exciting waves, τ_σ is the phase delay of the pitch moment relative to the heave force, $\bar{Z}_0$ is a measure of the amplitude of the heave force, and $\bar{\Theta}_0$ is a measure of the amplitude of the pitch moment. We note that $\bar{Z}_0$ and $\bar{\Theta}_0$ are functions of the wave height as well as the position of the mass centre in the wave. Equations (2.1) and (2.2) are uncoupled linear equations, and their solutions can be expressed as

$$z = a_z \cos(\Omega t + \tau_z), \tag{2.6}$$

$$\theta = a_\theta \cos(\Omega t + \tau_\theta), \tag{2.7}$$

where a_z and a_θ are the amplitudes of heave and pitch, respectively; τ_z and τ_θ are the phase lags of heave and pitch relative to the excitation wave; and τ_θ is a function of ζ_θ and τ_σ.

We consider the case in which the ship is in head waves so that $\bar{K}(t) = 0$ in equation (2.3). Substituting equations (2.6) and (2.7) into equation (2.3), we obtain

$$\ddot{\phi} + \omega_\phi^2 \phi + 2\mu_1 \dot{\phi} + 2\mu_3 \dot{\phi}^3 - \alpha_3 \phi^3 + [f_1 \cos(\Omega t + \tau_z) + f_3 \cos(\Omega t + \tau_\theta)]\phi + [f_2 \sin(\Omega t + \tau_z) + f_4 \sin(\Omega t + \tau_\theta)]\dot{\phi} = 0, \tag{2.8}$$

where

$$\left.\begin{aligned} f_1 &= -\tfrac{1}{2} a_z K_{\phi z}, & f_2 &= \tfrac{1}{2}\Omega a_z K_{\dot{\phi}\dot{z}}, \\ f_3 &= -\tfrac{1}{2} a_\theta K_{\phi\theta}, & f_4 &= \tfrac{1}{2}\Omega a_\theta K_{\dot{\phi}\dot{\theta}}. \end{aligned}\right\} \tag{2.9}$$

The straightforward expansion of the solution of equation (2.8) shows that resonances occur when $\Omega/\omega_\phi \approx 1, 2, 4, \ldots$. The first two cases are known as the fundamental and principal parametric resonances, respectively. Blocki (1980) concluded that the most dangerous case is principal resonance. Nayfeh & Sanchez (1990) presented the bifurcation diagram in terms of the frequency and amplitude of the excitation, and showed that the principal resonance occurs at the smallest excitation amplitude.

Using the method of multiple scales (Nayfeh 1973, 1981; Nayfeh & Mook 1979), Oh *et al*. (1992) found that, to the first approximation,

$$\phi(t) \approx a\cos[\tfrac{1}{2}(\Omega t - \gamma + \tau_f)], \tag{2.10}$$

where

$$\dot{a} = -\mu_1 a - \tfrac{3}{4}\mu_3\omega_\phi^2 a^3 - \frac{Fa}{2\omega_\phi}\sin\gamma \tag{2.11}$$

$$a\dot{\gamma} = a\sigma + \frac{3\alpha_3}{4\omega_\phi}a^3 - \frac{Fa}{\omega_\phi}\cos\gamma, \tag{2.12}$$

$$\Omega = 2\omega_\phi + \sigma, \tag{2.13}$$

and

$$\tfrac{1}{2}(f_1 e^{i\tau_z} - f_2\omega_\phi e^{i\tau_z} + f_3 e^{i\tau_\theta} - f_4\omega_\phi e^{i\tau_\theta}) = f e^{i\tau_f}. \tag{2.14}$$

Here, f is an effective amplitude, due to the combined influence of heave and pitch, and a complex function of $K_{\phi z}$, $K_{\phi\theta}$, $K_{\dot{\phi}\dot{z}}$, $K_{\dot{\phi}\dot{\theta}}$, a_z, a_θ, Ω, ω_ϕ, τ_z and τ_θ.

Periodic motions correspond to the fixed points of equations (2.11) and (2.12); that is $\dot{a} = 0$ and $\dot{\gamma} = 0$. There are two possibilities:

(1) $a = 0$ and the roll motion is not excited; and

(2) $a \neq 0$ and the roll motion is excited.

The stability of a given fixed point can be ascertained by investigating the eigenvalues of the linearized equations (2.11) and (2.12) evaluated at the fixed point.

In figure 1, we show a typical force–response curve for $\mu_1 = \mu_3 = 0.04$, $\alpha_3 = 1.0$, and $\sigma = 0.20$, which exhibits a supercritical pitchfork bifurcation. When $0 \leqslant f \leqslant \zeta_2 = 0.2155$, only the trivial solution exists, which is stable. When $f > \zeta_2$, there are two solutions: the trivial solution, which is unstable, and a non-trivial solution, which is stable. The value ζ_2 corresponds to a supercritical pitchfork bifurcation.

In figure 2, we show a typical force–response curve that exhibits a subcritical pitchfork bifurcation. The values of the parameters are the same as in figure 1, except that the sign of σ is reversed. In the interval $0 \leqslant f < \zeta_1 = 0.0957$, only the trivial solution exists, which is stable. When $f_1 \leqslant f < \zeta_2 = 0.2155$, there are three solutions: the trivial solution, which is stable, and two non-trivial solutions, of which the large one is stable and the small one is unstable. In an experiment, one would never see motion corresponding to the small non-trivial solution. However, one would expect to see one of two possible motions, either no roll (corresponding to the trivial solution) or a rather-large-amplitude roll. The initial conditions, or external disturbances, determine which motion develops. When $\zeta_2 < f$, there are two solutions: the trivial solution, which is unstable, and a non-trivial solution, which is stable. In this range, one would expect to see a large-amplitude rolling motion.

(*b*) *Experiments*

A series of experiments were conducted in the VPI & SU towing basin with a wooden model of a tanker. The model is *ca.* $223.5 \times 29.2 \times 19.1$ cm^3. The weight of the model and ballast is *ca.* 54.5 kg.

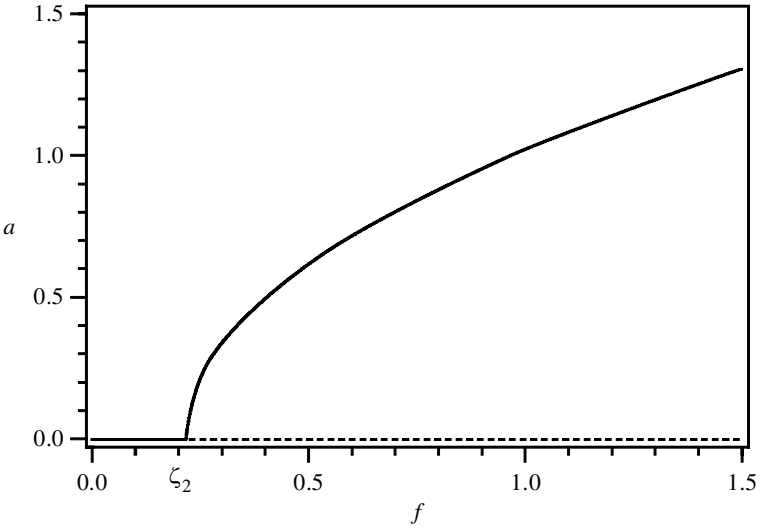

Figure 1. A force–response curve that exhibits a supercritical pitchfork bifurcation in the case of parametric resonance: $\mu_1 = \mu_3 = 0.04$, $\sigma = 0.20$, $\omega_\phi = 1$, $\alpha_3 = 1$, $f = 0.2155$; stable (——), unstable (– – –).

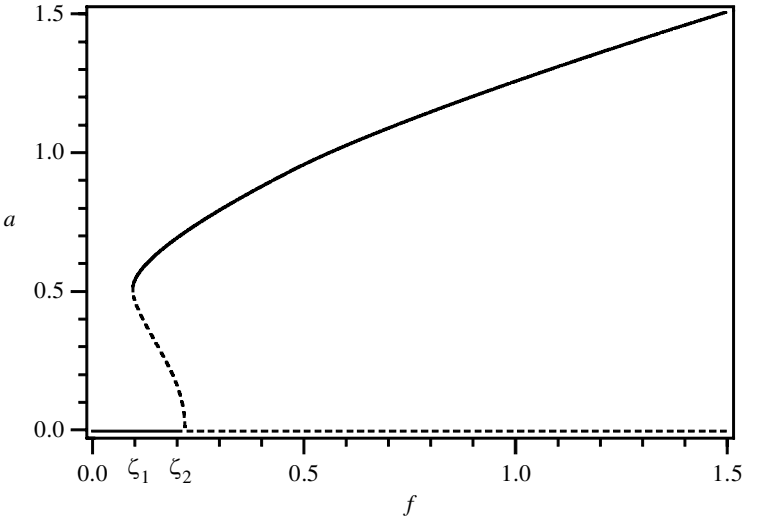

Figure 2. A force–response curve that exhibits a subcritical pitchfork bifurcation in the case of parametric resonance: $\mu_1 = \mu_3 = 0.04$, $\sigma = 0.20$, $\omega_\phi = 1$, $\alpha_3 = 1$, $f = 0.2155$; stable (——), unstable (– – –).

(*c*) *Experimental set-up*

The towing basin of the VPI & SU is *ca.* $30 \times 1.8 \times 2.5$ m^3. A plunger-type wavemaker consisting of a flat steel plate and hydraulic actuators is installed at one end. A set of wave absorbers is placed behind the wavemaker and another set is placed at the other end. There is a towing carriage on the rails of the basin, which was used as a stationary mounting platform for the model in the present experiment.

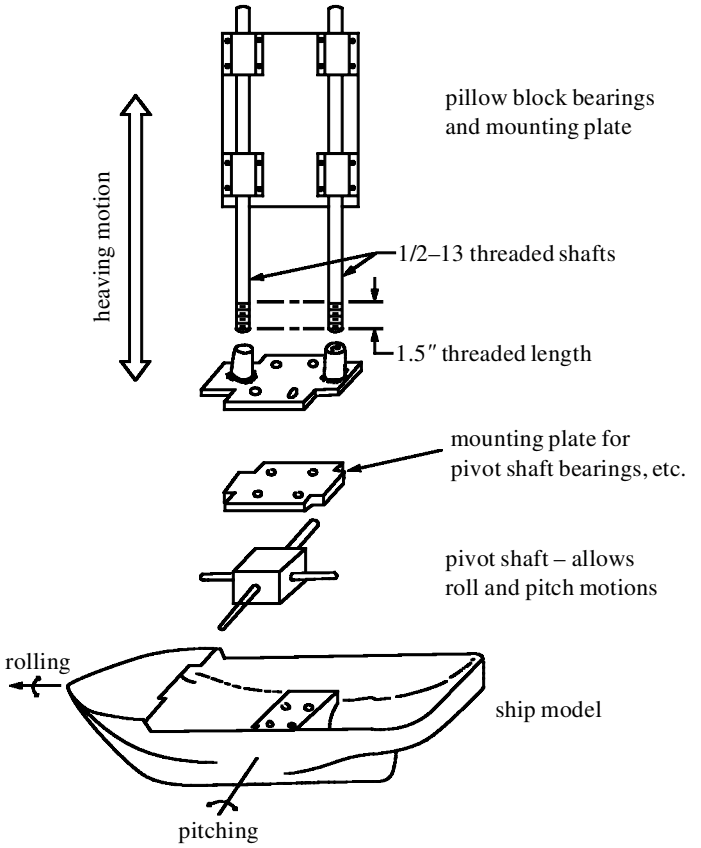

Figure 3. A schematic of the motion guidance system.

The model was free to move in heave, pitch and roll, while surge, sway and yaw were completely constrained. Pitch and roll motions were possible up to ±22° each. The support for the heave motion (figure 3) consisted of a pair of 1.27 cm-diameter hardened ground-steel rods and four linear bearings mounted on a steel plate. Heave motions were possible up to ±15.24 cm. The rotational apparatus was made of aluminium and consisted of two identical blocks and a pin-linkage system. It sat on Plexiglas shim plates at the floor of the model. A variety of shim plates was used to position the apparatus at the desired locations in the model. The linear-motion device was linked to the rotational-motion device at its bottom. The angular displacements in pitch and roll were measured by two RVDTs, which were fixed to the shafts of the rotational-motion apparatus. The heave displacement was measured by an LVDT, which was mounted on the supporting plate of the heave staffs and in the middle of the two heave rods.

The wave heights were measured using two capacitance-type gauges. One was mounted ahead of the bow and aligned with the centrelines of both the model and the towing tank. It could be moved around the towing tank. The locations of the peak amplitudes of the waves depended on the wave frequencies. The other was placed amidships to monitor reflected waves from the sidewalls of the towing tank. To control and monitor the movement of the wavemaker, a 61 cm LVDT was mounted

on its top and aligned with the driving piston. Its signal and the signal from the function generator were fed to the control box and an oscilloscope. The signal from the wavemaker contained high-frequency noise, which was *ca.* 180° out of phase with the signal from the function generator.

Two digital multimeters and a strip-chart recorder were used to monitor the responses of the model. An A/D converter was used, and data acquisition was done with a commercial software package. Data were stored on a personal computer. Two microprocessors analysed most of the data.

The essential sensors, such as the RVDTs, LVDTs, two wave-level gauges, and all the peripheral electronic instruments were calibrated before being installed to check the linearities and to obtain scale factors for the physical quantities.

(*d*) *Experimental procedure*

Tests were done without a model to map the frequencies and amplitudes for which the wavemaker produced plane waves. It was observed that operating the wavemaker at *ca.* 0.60 Hz produces plane waves for the widest range of amplitudes. Because interest was focused on the principal parametric resonance, weights were distributed inside the model so that its natural frequency in roll (*ca.* 0.32 Hz) was about half of the optimal frequency of the waves (*ca.* 0.6 Hz).

With the model in place, the wavemaker was started at the lowest amplitude available. The amplitude was then increased very slightly to the next step in the function generator, while the behaviour of the model in the waves and various signals were continuously monitored. A period ranging from 1/2 h to 4 h, depending on the amplitude and frequency of waves being generated, was required to achieve a steady state. After reaching the maximum amplitude of the waves available in the present experimental set-up, the wave amplitude was slowly decreased.

During this process, jumps up and down were observed, and the range of wave amplitudes where roll motions exist was obtained. When the jump up did not occur spontaneously, external disturbances of various kinds were imposed on the model at each step of the wave amplitude; these disturbances produced large-amplitude stable roll motion in many cases. Videotape recordings and/or photographs were made during the tests.

(*e*) *Results*

In figure 4, experimental force–response curves are shown. The arrows indicate the direction of sweep. As the wave amplitude was slowly increased, rolling did not occur until the wave height reached a certain critical value (ζ_2). Then large-amplitude rolling suddenly occurred (the jump-up phenomenon). When the wave amplitude was increased continuously beyond the jump-up bifurcation value (ζ_2), the amplitude of the roll motion remained almost constant or even decreased, instead of increasing monotonically as predicted by the theory.

After reaching the maximum height possible in our experimental set-up, the wave amplitude was slowly reduced. The large-amplitude rolling continued at wave heights below the jump-up bifurcation value (ζ_2). When the wave amplitude was decreased further to another critical value (ζ_1; $\zeta_1 < \zeta_2$), the large-amplitude rolling suddenly died out (the jump-down phenomenon), and no discernible rolling existed below ζ_1.

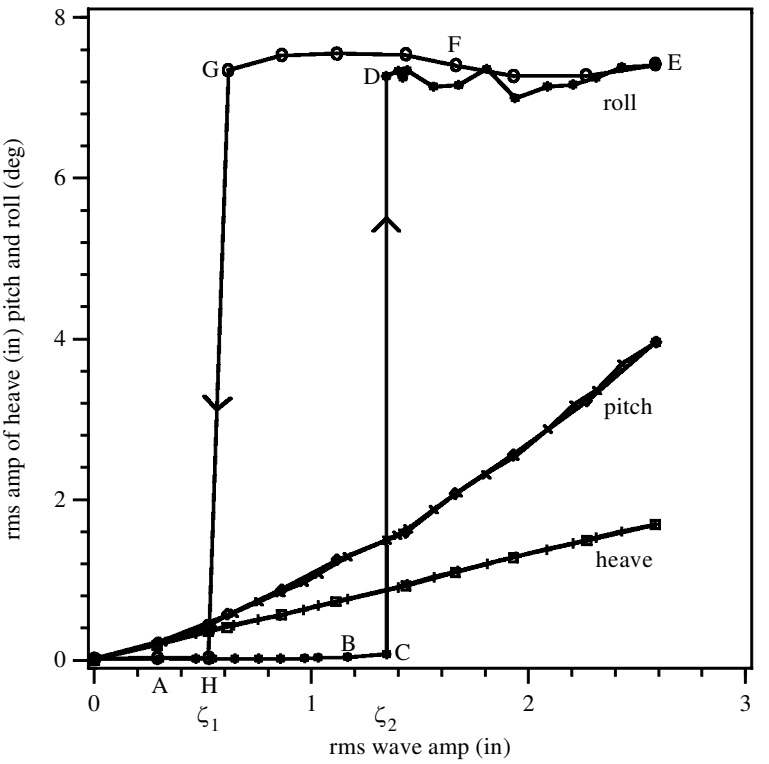

Figure 4. A typical experimentally obtained force–response curve in the case of parametric resonance for a wave frequency of 0.58 Hz; the model is at antinode 5 in figure 5.

In the range of wave amplitudes between the jump up (ζ_2) and jump down (ζ_1) bifurcation values, a stable non-rolling motion coexisted with a stable large-amplitude rolling motion, which was sometimes as large as $\pm 20°$. When the model was not exhibiting any noticeable roll, some disturbances in the roll mode could cause a jump up to large-amplitude steady-state rolling anywhere between ζ_1 and ζ_2. The domain of attraction (i.e. the set of disturbances) for large-amplitude rolling increased as the wave amplitude increased toward ζ_2. This subcritical type of instability was observed at all locations of the model in the standing waves for a wave frequency of 0.60 Hz.

The coexistence of two motions for the same wave pattern is evident in figure 4. The wave frequency is 0.60 Hz at location number 4 (see figure 5). The sequence of events is marked by arrows from A to H; A → H → B → C → D → E → F → G → H → A. The wave amplitude marked at point H corresponds to ζ_1, and the one at point C corresponds to ζ_2. Just after the wave amplitude passed point C, a sudden jump up to point D occurred. Thereafter, the roll-free motion was unstable and only the large-amplitude rolling was stable.

After point E, the wave amplitude was decreased slowly. The large-amplitude rolling existed below point D, where the jump up occurred during the sweep up. When the wave amplitude was decreased to slightly below G, a sudden jump down to point H occurred and rolling stopped. Between H and C, two different stable

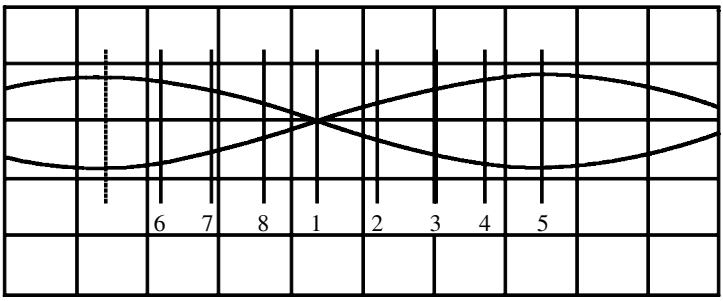

Figure 5. The various positions of the model in the wave. The centre of mass is positioned at the points numbered with respect to the wave.

motions exist: the non-rolling motion and the large-amplitude rolling. The motion that develops depends on the initial conditions. It was surprising to observe such large-amplitude rolling of the model in waves of such small amplitudes just before the jump down, but we recall that the theory predicts that small pitch and heave motions can excite relatively large rolling.

The responses in heave and pitch were nearly linear during the whole test, regardless of the magnitude of the roll response and the occurrence of jumps. In figures 6–8, fast Fourier transforms (FFTs) and time traces corresponding to three points on the curves in figure 4 are plotted. Figure 6 shows the FFTs and corresponding time signals at point B. The first harmonic components of all the responses of heave, pitch and roll are at the same frequency as the wave. The roll is not discernible with the naked eye there. Figure 7 corresponds to point D (i.e. just after the jump up). The roll response has the largest peak at half the frequency of the waves, which is a dramatic change from figure 6. The heave and pitch continue at the same frequency as the waves. In figure 8, plots of the responses at point H (i.e. just after the jump down) are shown. The large peak at half of the frequency of the waves disappeared and the slight rolling returned to the frequency of the waves. The magnitude of roll motion decreased drastically and was not noticeable with the naked eye.

(*f*) *Influence of modal position with respect to waves*

Experiments were also conducted to show the dependence of the response on the location of the centre of gravity of the model along a wavelength of the standing waves. These results are relevant to the questions of dynamic course instability and instability of the motion of a ship when it is navigating with the same speed as the waves, so that its encounter frequency is nearly zero.

The jump-up and jump-down bifurcation values (ζ_2) and (ζ_1) varied with the different positions of the model in the waves. These observations are consistent with the work of Renilson & Driscoll (1982). Renilson & Driscoll (1982) and Spyrou (1996*a*, *b*, 1997) concluded from experiments conducted in the large circulating water channel (CWC) at the National Maritime Institute that the motion, the magnitude and direction of the side force, and the possibility of a ship broaching while operating in slowly overtaking following or quartering regular waves, are dependent on its longitudinal position in the wave system. They actually considered the case of zero frequency of encounter. They found that a wave-induced longitudinal force could lead a ship to a steady-state position relative to the waves; at this point, the ship and the 'following'

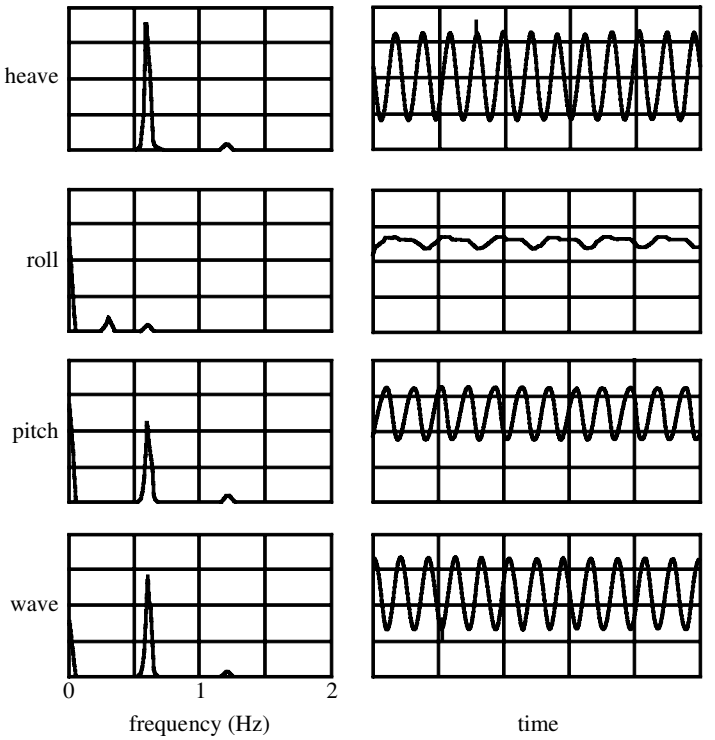

Figure 6. The spectra and time traces corresponding to point B in figure 4.

waves are moving at the same speed. They showed that the response of a ship varies over the wavelength, and that the effects of heel angle due to rolling motion can lead to course instability, such as broaching.

Spyrou (1996*a*) analysed the dynamic instability of a ship due to surf-riding in quartering seas (i.e. the situation in which the ship is forced to move with the wave due to the longitudinal wave force). He showed that the surf-riding states form a closed curve in state space and that fold and Hopf bifurcations take place. He explained the link between surf-riding and broaching on the basis of a homoclinic connection associated with surf-riding. He analysed the process of escape from surf-riding, and, on the basis of the final state of the ship, described the arrangement of the domains of broaching, capsizing, surf-riding and overtaking-wave periodic motion in the plane of Froude number and ship heading (Spyrou 1996*b*). He analysed a cumulative-type broaching that may occur when the speed of the ship is not close to that of the wave (Spyrou 1997). He identified a mechanism based on a period-doubling bifurcation followed by a jump to resonant yaw from a cyclic-fold bifurcation.

We placed the model at various positions along a wavelength of the same standing waves with a frequency of 0.60 Hz. The relative locations are numbered 1–8 in figure 5. The node is numbered 1, the antinode is 5, and so on. Changing the location of the ship along the wavelength changes the phase between the pitch and heave motions, and, hence, changes the effective amplitude of the parametric excitation of the roll mode.

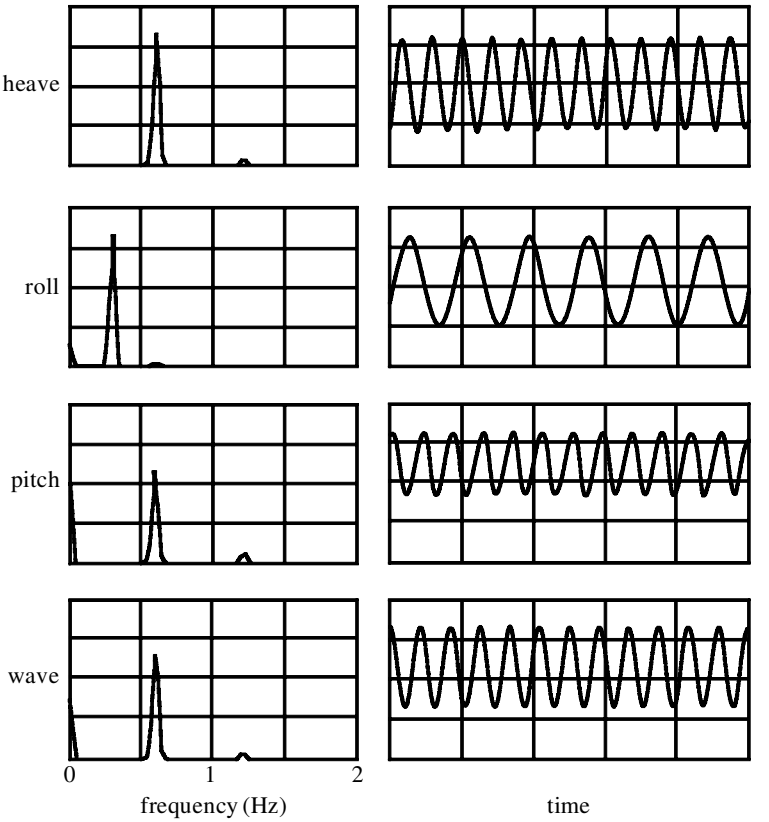

Figure 7. The spectra and time traces corresponding to point D in figure 4.

The results (Oh *et al*. 1992) show that the heave amplitude is proportional to the wave amplitude at a specific location along a wavelength of the standing waves, which is the linear response as expected. In other words, the heave amplitude is largest at the antinode (location number 5) where the wave amplitude is largest; the heave amplitude is smallest at the node (location number 1) where the wave amplitude is smallest; and the heave amplitudes at other locations can be arranged in proper downward order from antinode to node according to the wave amplitudes at specific locations. Moreover, the pitch amplitude is proportional to the wave slope at each specific location along a wavelength of the standing waves, which is also expected from the linear results. They are generally opposite in order to the heave responses: the pitch amplitude is largest at the node (location number 1) where the wave slope is largest; the pitch amplitude is smallest at the antinode (location number 5) where the wave slope is smallest; and the pitch amplitudes at other locations can be arranged in proper downward order from node to antinode according to the wave slopes at specific locations.

The effective amplitude of the parametric excitation of the roll mode is produced by the combined role of heave and pitch, and, hence, varies with the location of the centre of gravity in the wave form even when the wave frequency is fixed. Location number 2 produced the seventh largest heave amplitude out of the eight locations considered,

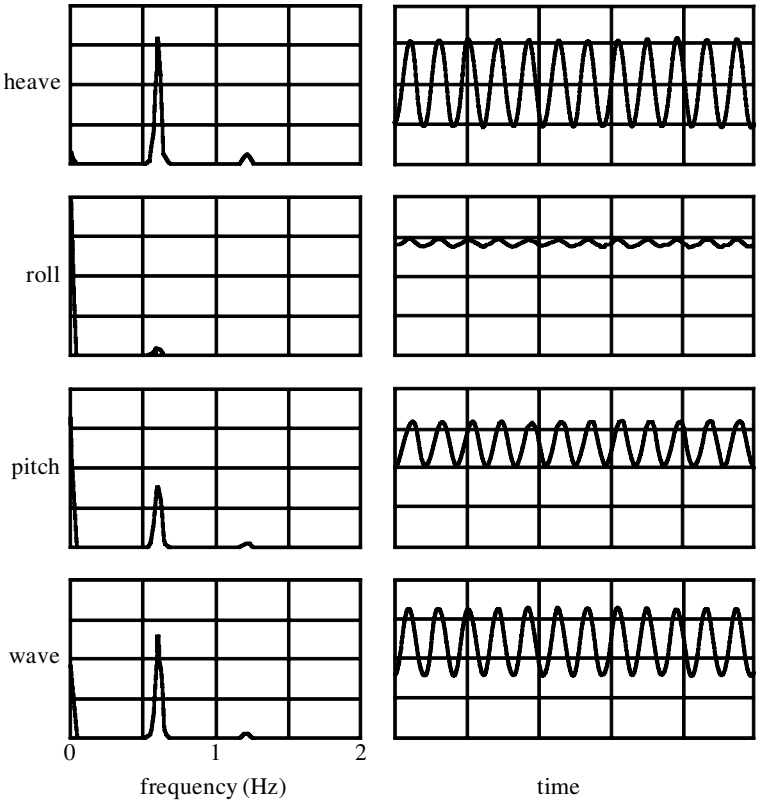

Figure 8. The spectra and time traces corresponding to point H in figure 4.

the second largest pitch amplitude, and the largest amplitude of the upper-branch roll motion. Location number 1 (the node) produced the smallest heave, the largest pitch, and the second largest roll amplitude. Location number 5 (the antinode) produced the largest heave, the smallest pitch, and the third largest roll amplitude. Location number 6 produced the second largest heave, the seventh largest pitch, and the smallest roll amplitude, and so on. Hence, the present study significantly extends the work of Blocki (1980) and Sanchez & Nayfeh (1990). In the real motion, the ship will necessarily experience pitch; therefore, the pitch mode should be included along with the heave in investigating the parametric resonance of the roll mode.

3. Autoparametric resonance

Strong coupling between pitch and roll was first mentioned by Froude in 1863. He observed that a vessel whose natural frequency in heave is twice its natural frequency in roll has undesirable seakeeping characteristics. For a century after Froude stated his observations, no research related to this phenomenon was pursued. Then Kerwin (1955), Paulling & Rosenberg (1959), Kinney (1961) and Blocki (1980) investigated the influence of a prescribed heave motion on the roll motion. Paulling & Rosenberg (1959) studied the effect of the two-to-one ratio of frequencies analytically and experimentally. They considered a model with only two degrees of freedom, heave

and roll. Then they considered the heave motion to be a prescribed simple-harmonic oscillation. In deriving the equation of motion for roll, they included a quadratic term to account for the roll–heave coupling, a product of the roll and heave displacements. Finally, because the heave motion was prescribed, they found that a linear Mathieu equation governed roll; the time-dependent coefficient was the function describing the heave motion in the quadratic term. Unsurprisingly, they found that roll could be excited by means of a parametric resonance. Of course, such an analysis predicted an infinitely growing roll motion.

In the analytical models mentioned above, heave influenced roll, but roll did not influence heave. The experimental models of Paulling & Rosenberg (1959) and Blocki (1980) were constructed to conform with the analysis. Their models were rigidly constrained to eliminate all degrees of freedom except roll and heave. A simple-harmonic heave oscillation was then impressed on the model, which otherwise was sitting in calm water. They observed heave-induced roll as predicted. The principal shortcoming of their study was that the heave motion was prescribed; hence, the effects of the roll motion and the waves on the heave motion were not taken into account.

During the last few decades, interest in the excitation of roll by heave and/or pitch, or, equivalently, head or following waves, has increased considerably. Nayfeh *et al*. (1973) and Mook *et al*. (1974) extended the model set of equations used by Paulling & Rosenberg (1959) by considering two nonlinearly coupled equations governing pitch and roll. In their equations, pitch is not prescribed but is coupled to the roll motion; consequently, the pitch (heave) and roll motions are determined simultaneously as functions of a prescribed wave motion. They explained the significance of the two-to-one ratio of frequencies in causing undesirable roll behaviours. Among other things they found the saturation phenomenon, jumps, and regions where periodic responses to periodic excitations do not exist.

Nayfeh (1988) considered the nonlinearly coupled roll and pitch motions of a ship in regular head waves. The coupling is through hydrostatic terms. The pitch frequency is approximately twice the roll frequency, and the encounter frequency is near to either the pitch or the roll natural frequency. He found the saturation phenomenon when the encounter frequency is near the pitch natural frequency and the existence of Hopf bifurcations and, hence, complicated motions. Nayfeh & Oh (1995) extended the work of Nayfeh (1988) by using a linear-plus-quadratic damping model for roll and investigated the case of primary resonance for pitch. They found supercritical and subcritical instabilities, periodic motions, periodically and chaotically modulated motions, period-doubling bifurcations, and the coexistence of multiple solutions and associated jumps. The quadratic damping eliminated the saturation phenomenon.

(*a*) *Theoretical analysis*

In this section, we summarize the results of Nayfeh (1988), and Nayfeh & Oh (1995) for the case $\Omega = 2\omega_2 + \sigma_2$ and $\omega_2 = 2\omega_1 + \sigma_1$.

We consider a ship that is restricted to pitch and roll and study its response to a regular sea. We assume that the ship is laterally symmetric. We introduce a body-fixed coordinate system Oxyz such that its origin O is at the centre of mass, the x-axis is positive toward the bow, the y-axis is positive toward starboard, and the z-axis is positive downward. The orientation of the ship with respect to an inertial

frame $OXYZ$ is defined by the Euler angles ϕ and θ as follows: θ is a pitch-like rotation about the original y-axis, and ϕ is a roll-like rotation about the new x-axis. The components p and q of the angular velocity about the x- and y-axes are related to ϕ, θ, $\dot{\phi}$ and $\dot{\theta}$ by

$$p = \dot{\phi} \quad \text{and} \quad q = \dot{\theta}\cos\phi. \tag{3.1}$$

The equations of motion can be written as

$$I_{xx}\dot{p} - I_{xz}pq = K + K_0\cos\Omega t, \tag{3.2}$$

$$I_{yy}\dot{q} + I_{xz}p^2 = M + M_0\cos(\Omega t + \tau), \tag{3.3}$$

where I_{xx}, I_{yy} and I_{xz} are the moments and product of inertia, Ω is the encounter frequency, K_0 and M_0 are the amplitudes of the moments produced by the waves, and τ is a phase; all are assumed to be constants. Assuming the hydrodynamic moments K and M to be analytic functions of ϕ and θ and their derivatives, taking symmetry into account, adding a quadratic roll damping term, and eliminating interactions between first and second derivatives as well as terms that are quadratic in the second derivatives, we obtain

$$\begin{aligned} K = {} & K_\phi\phi + K_{\dot\phi}\dot{\phi} + K_{\ddot\phi}\ddot{\phi} + K_{\phi\theta}\phi\theta + K_{\phi\dot\theta}\phi\dot{\theta} + K_{\phi\ddot\theta}\phi\ddot{\theta} \\ & + K_{\theta\dot\phi}\theta\dot{\phi} + K_{\theta\ddot\phi}\theta\ddot{\phi} + K_{\dot\phi\dot\theta}\dot{\phi}\dot{\theta} - K_{\dot\phi\dot\phi}\dot{\phi}\mid\dot{\phi}\mid + \text{cubic terms}, \end{aligned} \tag{3.4}$$

$$\begin{aligned} M = {} & M_\theta\theta + M_{\dot\theta}\dot{\theta} + M_{\ddot\theta}\ddot{\theta} + \tfrac{1}{2}M_{\phi\phi}\phi^2 + M_{\phi\dot\phi}\phi\dot{\phi} + M_{\phi\ddot\phi}\phi\ddot{\phi} \\ & + \tfrac{1}{2}M_{\theta\theta}\theta^2 + M_{\theta\dot\theta}\theta\dot{\theta} + M_{\theta\ddot\theta}\theta\ddot{\theta} + \tfrac{1}{2}M_{\dot\phi\dot\phi}\dot{\phi}^2 + \tfrac{1}{2}M_{\dot\theta\dot\theta}\dot{\theta}^2 + \text{cubic terms}, \end{aligned} \tag{3.5}$$

where the stability derivatives must be obtained from other considerations. Nayfeh *et al.* (1973, 1974) showed that self-sustained ship oscillations exist unless the following relations are satisfied:

$$K_{\phi\dot\theta} = K_{\theta\dot\phi} = M_{\phi\dot\phi} = M_{\theta\dot\theta} = 0, \tag{3.6}$$

$$K_{\phi\theta} = M_{\phi\phi}, \tag{3.7}$$

$$K_{\theta\ddot\phi} + 4K_{\phi\ddot\theta} - 2K_{\dot\phi\dot\theta} = M_{\dot\phi\dot\phi} + 2M_{\phi\ddot\phi}. \tag{3.8}$$

Substituting equations (3.1) and (3.4)–(3.8) into equations (3.2) and (3.3), and noting that $q = \dot{\theta} + \text{cubic terms}$, we obtain

$$\ddot{\phi} + \omega_1^2\phi = -2\mu_1\dot{\phi} - \mu_3\dot{\phi}\mid\dot{\phi}\mid + \delta_1\phi\theta + \delta_2\phi\ddot{\theta} + \delta_3\theta\ddot{\phi} + \delta_4\dot{\phi}\dot{\theta} + F_1\cos\Omega t, \tag{3.9}$$

$$\ddot{\theta} + \omega_2^2\theta = -2\mu_2\dot{\theta} + \alpha_1\phi^2 + \alpha_2\phi\ddot{\phi} + \alpha_3\theta^2 + \alpha_4\theta\ddot{\theta} + \alpha_5\dot{\phi}^2 + \alpha_6\dot{\theta}^2 + F_2\cos(\Omega t + \tau), \tag{3.10}$$

where

$$\begin{aligned} & \{\omega_1^2, 2\mu_1, \delta_1, \delta_2, \delta_3, \delta_4, F_1\} \\ & \quad = [I_{xx} - K_{\ddot\phi}]^{-1}\{-K_\phi, -K_{\dot\phi}, K_{\phi\theta}, K_{\phi\ddot\theta}, K_{\theta\ddot\phi}, K_{\dot\phi\dot\theta} + I_{xz}, K_0\}, \end{aligned} \tag{3.11}$$

$$\begin{aligned} & \{\omega_2^2, 2\mu_2, \alpha_1, \alpha_2, \alpha_3, \alpha_4, \alpha_5, \alpha_6, F_2\} \\ & \quad = [I_{yy} - M_{\ddot\theta}]^{-1}\{-M_\theta, -M_{\dot\theta}, \tfrac{1}{2}M_{\phi\phi}, M_{\dot\phi\dot\phi}, \tfrac{1}{2}M_{\theta\theta}, M_{\theta\dot\theta}, \tfrac{1}{2}M_{\dot\phi\dot\phi} - I_{xz}, \tfrac{1}{2}M_{\dot\theta\dot\theta}, M_0\}. \end{aligned} \tag{3.12}$$

Using the method of multiple scales (Nayfeh 1973, 1981; Nayfeh & Mook 1979), Nayfeh (1988), and Nayfeh & Oh (1995) obtained an approximate solution of equations (3.9) and (3.10) in the form

$$\phi = a_1 \cos(\tfrac{1}{2}\Omega t - \tfrac{1}{2}\gamma_1 - \tfrac{1}{2}\gamma_2 + \tfrac{1}{2}\tau), \tag{3.13}$$

$$\theta = a_2 \cos(\Omega t - \gamma_2 + \tau), \tag{3.14}$$

where

$$\dot{a}_1 = -\mu_1 a_1 + \Lambda_1 a_1 a_2 \sin\gamma_1 - \frac{4\mu_3\omega_1}{3\pi} a_1|a_1|, \tag{3.15}$$

$$\dot{a}_2 = -\mu_2 a_2 - \Lambda_2 a_1^2 \sin\gamma_1 + f\sin\gamma_2, \tag{3.16}$$

$$a_1\dot{\beta}_1 = -\Lambda_1 a_1 a_2 \cos\gamma_1, \tag{3.17}$$

$$a_2\dot{\beta}_2 = -\Lambda_2 a_1^2 \cos\gamma_1 - f\cos\gamma_2, \tag{3.18}$$

and

$$4\omega_1\Lambda_1 = \delta_1 - \omega_2^2\delta_2 - \omega_1^2\delta_3 + \omega_1\omega_2\delta_4, \tag{3.19}$$

$$4\omega_2\Lambda_2 = \alpha_1 - \omega_1^2(\alpha_2 + \alpha_5), \tag{3.20}$$

$$\omega_2 f = \tfrac{1}{2}F_2, \tag{3.21}$$

$$\gamma_1 = \sigma_1 t + \beta_2 - 2\beta_1 \quad \text{and} \quad \gamma_2 = \sigma_2 t - \beta_2 + \tau. \tag{3.22}$$

Periodic motions correspond to $a_i' = 0$ and $\gamma_i' = 0$; that is, to the fixed points of equations (3.15)–(3.18) and (3.22). There are two possibilities. Firstly,

$$a_1 = 0 \quad \text{and} \quad a_2 = \frac{f\sqrt{\Lambda_1}}{\sqrt{\sigma_2^2 + \mu_2^2}} \tag{3.23}$$

and the response is given by

$$\phi = 0 \quad \text{and} \quad \theta = a_2\cos(\Omega t + \tau - \gamma_2) + \cdots, \tag{3.24}$$

which is essentially the linear solution. Secondly,

$$a_2 = \sqrt{\Lambda_1}\left[\tfrac{1}{4}(\sigma_1 + \sigma_2)^2 + \left(\mu_1 + \frac{4\mu_3\omega_1\sqrt{\Lambda_2}}{3\pi}a_1\right)^2\right]^{1/2}, \tag{3.25}$$

and $a_1\sqrt{\Lambda_2} = x$ is given by the algebraic equation

$$x^4 + c_3 x|x| + c_2 x^2 + c_1 x + c_0 = 0, \tag{3.26}$$

where

$$c_0 = (\mu_2^2 + \sigma_2^2)[\tfrac{1}{4}(\sigma_1 + \sigma_2)^2 + \mu_1^2] - f^2,$$

$$c_1 = (\mu_2^2 + \sigma_2^2)\frac{8\mu_1\mu_3\omega_1}{3\pi},$$

$$c_2 = (\mu_2^2 + \sigma_2^2)\left(\frac{4\mu_3\omega_1}{3\pi}\right)^2 + 2\mu_1\mu_2 - \sigma_2(\sigma_1 + \sigma_2),$$

$$c_3 = \frac{8\mu_2\mu_3\omega_1}{3\pi}.$$

The response in this case is given by equations (3.13) and (3.14).

When $\mu_3 = 0$ but $a_1 \neq 0$, equation (3.25) becomes

$$a_2 = \sqrt{\Lambda_1}[\tfrac{1}{4}(\sigma_1 + \sigma_2)^2 + \mu_1^2]^{1/2} = a_2^*, \tag{3.27}$$

which is independent of a_1 and f. Moreover, $c_1 = c_3 = 0$, and, hence,

$$a_1 = \sqrt{\Lambda_2}[\Gamma_1 \pm (f^2 - \Gamma_2^2)^{1/2}]^{1/2}, \tag{3.28}$$

where

$$\Gamma_1 = \tfrac{1}{2}\sigma_2(\sigma_1 + \sigma_2) - \mu_1\mu_2, \tag{3.29}$$

$$\Gamma_2 = \sigma_2\mu_1 + \tfrac{1}{2}\mu_2(\sigma_1 + \sigma_2). \tag{3.30}$$

The solution does not exhibit the saturation phenomenon unless $\mu_3 = 0$. Instead, the amplitude a_2 of the directly excited pitch mode, as well as the amplitude a_1 of the roll mode, vary as functions of f. The stability of a given fixed point can be ascertained by investigating solutions of the variational equations (3.15)–(3.18) and (3.22) around the fixed point.

In figure 9, we show the variation of a_1 and a_2 with f for $\Lambda_1 = 1.0$, $\Lambda_2 = 0.5$, $\sigma_1 = 0.3$, $\sigma_2 = 0.1$, $\mu_1 = 0.2$, $\mu_2 = 0.5$ and $\mu_3 = 0.6$. In this case, $\Gamma_1 = -0.04$ and, hence, equation (3.28) has one real root when $f \geqslant \zeta_2$, where $\zeta_2 \approx 0.1649$. Consequently, when $f_2 \leqslant \zeta_2$, the response is given by equation (3.24); the roll mode is not excited because $a_1 = 0$, and the pitch mode is linearly excited because a_2 is given by equation (3.23). When $\mu_3 = 0$ and $f > \zeta_2$, the response is given by equations (3.13) and (3.14), where $a_2 = a_2^* = 0.2828 = \text{const.}$ for all values of f greater than ζ_2, and a_1 is given by equation (3.26). Hence, if an experiment is performed by setting $\Omega \approx \omega_2$ and the detunings and damping coefficients are such that $\Gamma_1 < 0$, one expects the pitch mode to dominate. This is initially so. But as f increases beyond the critical value ζ_2, a_2 remains constant and equal to a_2^* (that is, the pitch mode saturates) and the extra energy is spilled over into the roll mode. The saturation value a_2^* can be very small if $\sigma_1 + \sigma_2$ and μ_1 are small. The saturation phenomenon was first discovered by Nayfeh *et al.* (1973).

When $\mu_3 \neq 0$, the amplitude a_2 of the pitch mode no longer exhibits the saturation phenomenon. Instead, the amplitude a_2 of the pitch mode grows nonlinearly rather than staying at a constant value a_2^* as f increases beyond ζ_2. However, the slope of a_2 for $f \geqslant \zeta_2$ is still much less than that which corresponds to the case of linear damping. With the introduction of the quadratic damping, the rate of increase of the amplitude a_1 of the roll mode with f is less than that in the case of $\mu_3 = 0$. Consequently, as f increases beyond the bifurcation point ζ_2, not all the extra energy input to the pitch mode is spilled over into the roll mode.

In figure 10, we show typical force–response curves when $\mu_1 = \mu_2 = 0.04$ and $\sigma_1 = \sigma_2 = 0.5$ for $\mu_3 = 0.6$ and $\mu_3 = 0$. In this case, equation (3.28) has only one stable real root for $f \geqslant \zeta_2$ ($\zeta_2 \approx 0.2517$); two real roots for $\zeta_1 \leqslant f \leqslant \zeta_2$, where $\zeta_1 \approx 0.04$ when $\mu_3 = 0$ and $\zeta_1 \approx 0.1020$ when $\mu_3 = 0.6$. In the latter case, the large root is stable and the small one is unstable. The large bifurcation value ζ_2 is a subcritical pitchfork and is independent of the value of μ_3; the small bifurcation value ζ_1 is a saddle-node and increases as μ_3 increases. When $f \leqslant \zeta_1$, there exists only one stable response given by equation (3.23), which is linear and consists solely of the pitch mode. When $\zeta_1 \leqslant f \leqslant \zeta_2$, two stable solutions coexist with an unstable solution; one of the stable responses is given by equation (3.23), and the other stable

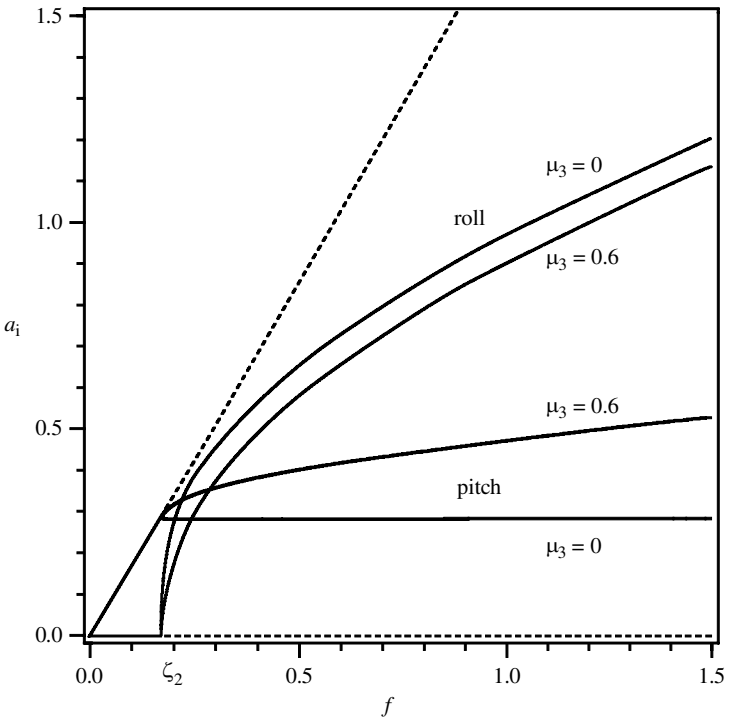

Figure 9. A force–response curve that exhibits a supercritical pitchfork bifurcation in the case of autoparametric resonance for $\mu_3 = 0$ and 0.6; stable (——), unstable (– – –).

solution is given by equations (3.25) and (3.26). The response of the ship in this region depends on the initial conditions. When $f \geqslant \zeta_2$, there exists only one stable response, again given by equations (3.25) and (3.26). The response of the roll mode exhibits the coexistence of two stable motions and the associated jump phenomenon for both $\mu_3 = 0$ and $\mu_3 = 0.6$. The saturation phenomenon, which exists when $\mu_3 = 0$, does not exist when $\mu_3 = 0.6$. When $\mu_3 = 0.6$, the amplitude a_2 of the pitch mode grows rather than remains constant as f increases beyond ζ_2. Again, for $f \geqslant \zeta_1$, a_2 increases and a_1 decreases as μ_3 increases.

Nayfeh & Oh (1995) found conditions for which the fixed points of the modulation equations undergo a Hopf bifurcation as one of the control parameters is varied. After the Hopf bifurcation occurs, amplitudes and phases of both the pitch and roll modes are modulated. The modulation may be periodic or chaotic. The Hopf bifurcation can be either subcritical or supercritical.

The bifurcated periodic solutions were found by a numerical algorithm, and Floquet theory was used to analyse their stability. The limit cycles deform and lose stability by either pitchfork or period-doubling bifurcations as either the encounter frequency or the excitation amplitude is varied. The pitchfork bifurcation breaks the symmetry of the limit cycle. The period-doubling bifurcations culminate in chaos. Nayfeh & Oh (1995) characterized the different possible solutions (limit cycles and chaotic attractors) using phase portraits, Poincaré sections, fast Fourier transforms, and time traces. The chaotic solutions exhibit very irregular behaviour with broadband spectra.

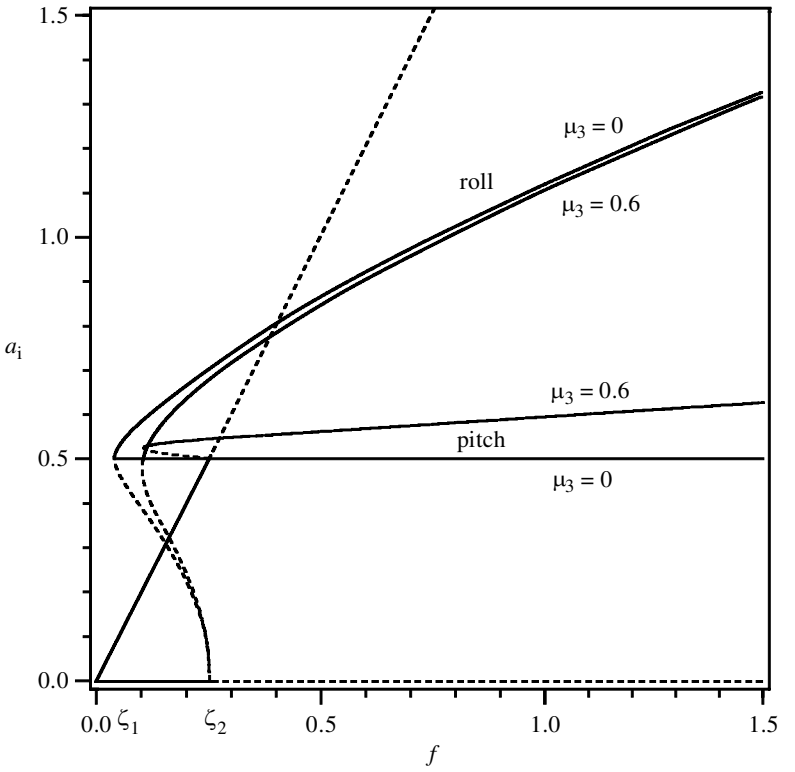

Figure 10. A force–response curve that exhibits a subcritical bifurcation in the case of autoparametric resonance for $\mu_3 = 0$ and 0.6; stable (——), unstable (– – –).

(*b*) *Experiments*

Experiments were conducted on a destroyer model in the towing basin at VPI & SU, described in § 2 *b*.

(*c*) *Description of the model*

The model, hull no. 4794, is of a US Navy destroyer, similar in form to a contemporary KNOX class ASW frigate. The model was constructed and used by the Carderock Division of the Naval Surface Warfare Research Center for resistance and seakeeping studies during the 1960s. Because of its age, a data sheet with normal model details and specifications (i.e. scale ratio, full-scale dimensions, appendage locations, moments of inertia) is not available. The hull does not have a rudder, sonar dome, bilge keels or a propeller. Its principal particulars, as measured, are $B_{\max} = 29.21$ cm, $D = 22.86$ cm, displacement = 54.5 kg at design waterline (DWL), $L_{OA} = 315$ cm, $d_a = d_f = d_m = 10.16$ cm, trim = 0.0 and $L/B = 10.78$.

The model was constructed from common pine. The interior was hollowed out to a large extent. This feature is extremely useful because additional weight can be distributed inside the model to produce the desired moments of inertia.

The measured natural frequencies of the unballasted model are 1.65 Hz in pitch, 1.45 Hz in heave, and 1.40 Hz in roll. Because the VPI & SU towing basin produces

the best smooth, regular, plane waves at *ca.* 0.60 Hz, the most desirable two-to-one ratio of natural frequencies for the model is a pitch or heave frequency of 0.60 Hz and a roll frequency of 0.30 Hz. We attempted to ballast the model to its DWL and simultaneously lower either the natural frequency of heave from 1.45 to 0.60 Hz or that of pitch from 1.65 to 0.60 Hz. The lowest heave natural frequency achievable with the model at the DWL is 1.26 Hz and that of pitch is 0.91 Hz; thus, it was impossible to achieve optimal conditions. Consequently, with the natural frequency for pitch adjusted to 0.91 Hz, the natural frequency for roll was adjusted to be *ca.* 0.46 Hz. The model was excited in the pitch mode by waves having frequencies between 0.85 and 0.95 Hz. The wave heights achievable at these frequencies are considerably less than those achievable at 0.6 Hz, but it turned out that the roll mode could be indirectly excited by either the pitch or the heave mode, in the presence of a two-to-one internal resonance, with relatively low-amplitude waves.

During the first stages of the research, the goal was simply to allow the model to move with two degrees of freedom: roll and pitch. However, later it was decided to include heave, which is the most prominent motion of a floating body. Furthermore, for large-amplitude longitudinal waves, sway, yaw and, possibly, broaching occur concurrently with roll motion, as pointed out by Taggart & Kobayashi (1970) and Eda *et al.* (1979). However, in the present experiments, these motions were constrained.

Adjusting the natural frequencies is a painstaking process, because, if one characteristic parameter is varied, all the others vary simultaneously, and the centre of gravity of the weights and model must be remeasured. Many iterations are required. To achieve the desired natural frequencies, we configured the added weight as follows. Three compartments were built inside the model, two forward and one aft. Each compartment was filled with 9–11 kg of lead shot. A 2.3 kg weight was placed aft at the top of the stern deck, and another was placed forward. The forward weight was fitted on a threaded vertical rod that spans the distance from the keel to the main deck. This arrangement allowed the vertical position of the centre of gravity to be varied without changing its horizontal position and total displacement. Therefore, detuning the pitch and roll natural frequencies from the two-to-one ratio could be readily accomplished for a given displacement.

First we used a stopwatch to roughly check the natural frequency of each mode with the model floating on the calm water of the towing basin. We then mounted the model under the towing carriage and connected the cables of the motion-measuring transducers with the data-acquisition instruments and spectrum analysers. We then gave the model initial displacements to generate free oscillations and analysed these data with the spectrum analysers. The model was tuned until the desired natural frequencies, trim and waterline were reached.

The parameters used in one of the tests were $\omega_\phi = 0.495$ Hz, $\omega_\theta = 0.910$ Hz and $\Omega = 0.900$. Hence,

$$\sigma_1 = \omega_\theta - 2\omega_\phi = -0.08 \quad \text{and} \quad \sigma_2 = \Omega - \omega_\theta = -0.01.$$

(*d*) *Force–response curve*

In the theory, the amplitude and frequency of the waves are used as control parameters. Either the excitation amplitude is varied slowly while the frequency is kept constant, or the excitation frequency is varied slowly while the amplitude is kept constant. In either case, the response of concern is the steady state.

The duration of just one set of tests was as long as 10 days. Steady-state wave conditions in the basin often require very long times to develop, as much as several hours, for the following reasons. Firstly, in a fluid with low viscosity, such as water, transients need a long time to disappear; and secondly, because the water is contained in a confined space, the reflected waves interact with the newly generated components. The second effect is strong just after the parameter change. Consequently, we found it to be practically impossible to vary the frequency of a wave while keeping its amplitude constant. Accordingly, we restricted the experiment: the amplitude was slowly varied while the frequency was kept constant. Hence, we obtained only force–response curves.

The primary findings of the present work are the subcritical instability and associated jump phenomena. The experiments were focused on capturing the critical wave amplitudes at which large-amplitude roll motions occur and disappear. To obtain the force–response curves, we swept the wave amplitude up and down through the range where regular plane waves are generated.

In typical sweep-up and sweep-down processes, the jump phenomenon, the subcritical instability, and the coexistence of multiple responses to the same excitation were observed. These results are in good qualitative agreement with the theoretical results predicted in Nayfeh & Oh (1995). If a large-amplitude roll motion did not occur spontaneously during the sweep-up/sweep-down process, various external disturbances were imposed on the model in an attempt to obtain any coexisting large-amplitude roll motion.

In figure 11, we show a typical force–response curve exhibiting a subcritical pitchfork bifurcation obtained from the present experiments. These experimental results are consistent with the results predicted in Nayfeh & Oh (1995). A comparison of figures 10 and 11 reveals many similarities:

(a) the subcritical instability;

(b) the coexistence of large-amplitude and trivial roll motions;

(c) the associated jump phenomena in the range between the two bifurcation points ζ_1 and ζ_2 of the wave amplitude, as shown in figure 8, and the points L and C in figure 11;

(d) the breaking of the saturation phenomenon; and

(e) the nonlinear growth of the directly excited pitch mode.

In figure 11, the sweep-up process covers the increase in wave amplitude from point A to point H, and the sweep-down process covers the decrease in wave amplitude from point H to points L and A. The sequence of events is marked by arrows and capital letters from $\mathrm{A} \rightarrow \mathrm{B} \rightarrow \cdots \rightarrow \mathrm{K} \rightarrow \mathrm{L} \rightarrow \mathrm{A}$. As the excitation amplitude was increased slowly from A to C, only roll-free motion existed. The wave amplitude at point L corresponds to ζ_1, and at point C it corresponds to ζ_2 in figure 10.

A jump up was observed as the excitation amplitude exceeded a critical value, denoted by point C. This jump led to a large-amplitude roll motion. The jump-up point is marked as point D. To ascertain the stability of the large-amplitude roll response, we constrained the model to have a roll-free response. However, when the constraint was removed from the model, the response returned to the large-amplitude

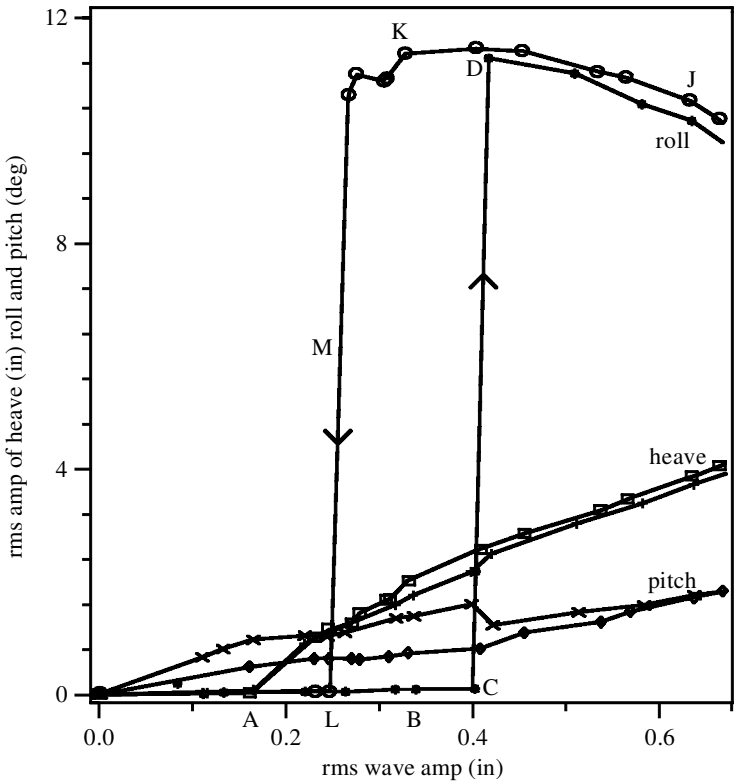

Figure 11. A typical experimentally obtained force–response curve in the case of autoparametric resonance for a wave frequency of 0.91 Hz; the model is at antinode 5 in figure 5.

roll motion. The time traces and the spectra of the roll, pitch, heave and wave motions are shown in figures 12 and 13, respectively corresponding to points B and D. It is very clear from these figures that there are no significant changes in the pitch, heave, and excitation signals. However, the roll signal displays drastic changes: firstly, the roll amplitude has increased to a very large value (note the scales of the plots); secondly, in the FFT results, the largest peak of the roll appears at the subharmonic of order one-half, while the largest peaks of the pitch and heave are at the wave frequency.

When the excitation amplitude was increased further from point D to E, the roll amplitude did not increase; instead it decreased, which is inconsistent with the theoretical result given in figure 10.

In the sweep down, as the wave amplitude was decreased from point J, the response became similar to the one at point D. As the wave amplitude was further reduced from point J to point K, the large-amplitude roll motion continued below the wave amplitude at which the upward jump occurred. This is the subcritical instability. The roll amplitude increased gradually and then decreased; in this interval, the shape of the experimental force–response curve resembles the one predicted by the theory (figure 10). In figure 14 the results are shown for point K, where the roll amplitude is the largest among the cases considered so far along the curve. We also note that at point K the roll amplitude is very large, up to $\pm 18^\circ$, while the amplitudes of the

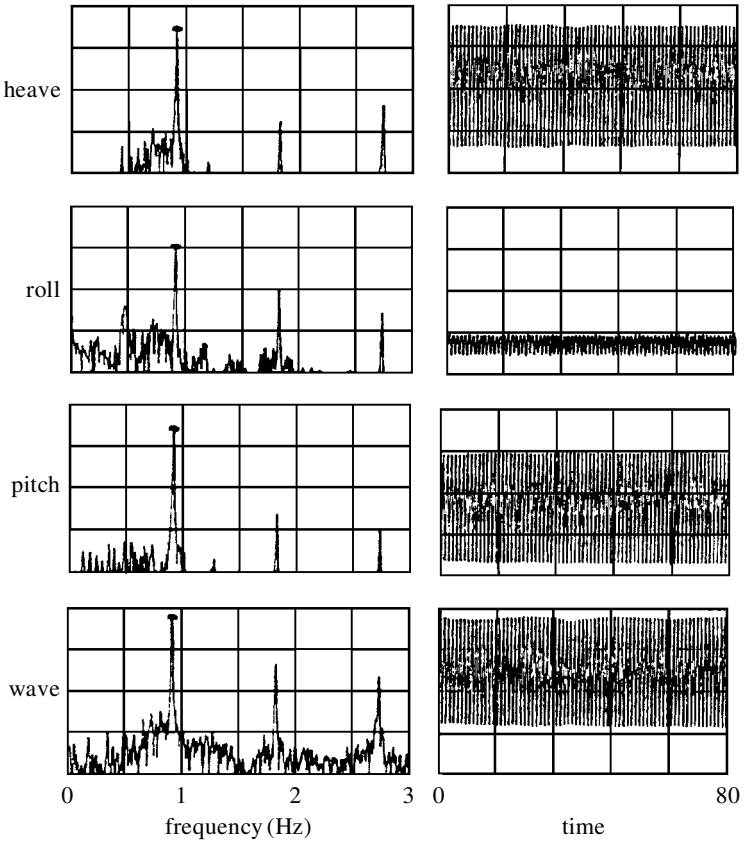

Figure 12. The spectra and time traces corresponding to point B in figure 11.

pitch, heave and wave are much smaller than those at points D and J. If one could observe the model for conditions corresponding to point K, one would be surprised that the model has such a large-amplitude roll in response to such a small wave.

When the excitation amplitude was slightly decreased below point K, a dramatic change occurred: the large-amplitude roll motion suddenly disappeared in a downward jump from a stable large-amplitude roll response to a stable roll-free response (from point K to point L).

It is difficult to predict when the upward and downward jumps in roll occur. They occur suddenly and the transitions passed so quickly that we were usually unable to acquire the digitized data. However, one downward jump was captured in digitized form, and the time traces and spectra for pitch and roll are presented in figure 15. One sees that the roll motion changed very sharply and that the pitch motion changed only slightly. The upward jump is similar except that the right-hand and left-hand sides of the time traces would be reversed.

During the entire sweep-up and sweep-down processes, the heave exhibited simple linear behaviour, regardless of the roll response, and the pitch exhibited neither linear nor saturated behaviour. This is in accord with theory (Nayfeh & Oh 1995). This result implies that initially, as the wave energy was fed into the pitch mode, the pitch response grew linearly with wave amplitude, while the roll remained very small. When

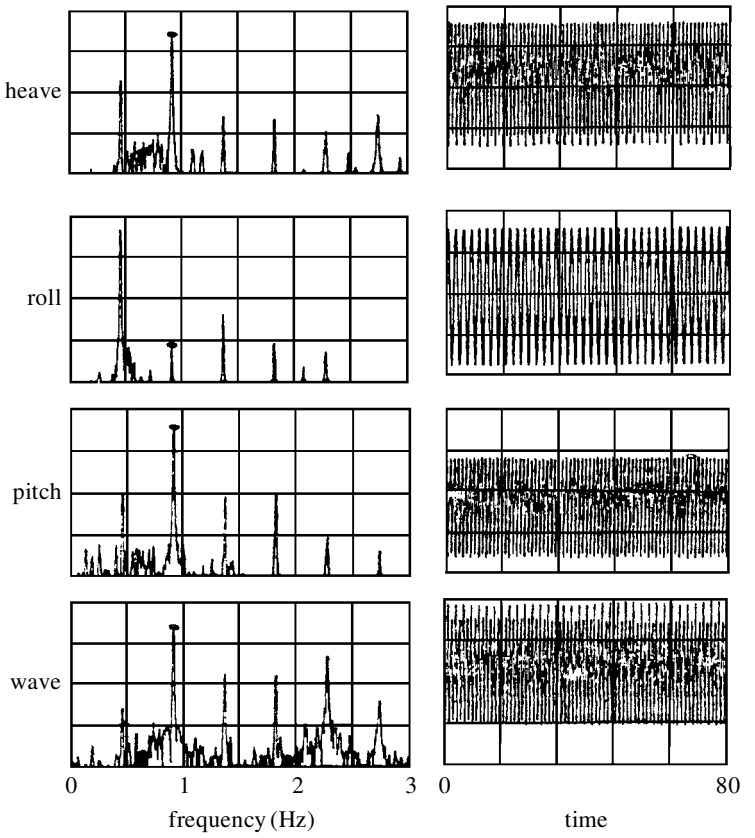

Figure 13. The spectra and time traces corresponding to point D in figure 11.

the wave amplitude increased beyond a certain critical value, the pitch response grew nonlinearly with wave amplitude, with its growth rate being much smaller than the linear rate, and the roll mode acquired a large amplitude. Thus, beyond the critical wave amplitude, a significant portion of the input energy was spilled over into the roll mode, while the small remaining portion increased the amplitude of the pitch mode slightly above the amplitude in the saturated case.

The energy transfer from the pitch mode to the roll mode is due to strong nonlinear couplings between these modes. The strong couplings are the result of the two-to-one ratio of natural frequencies, which produces an internal resonance. Because of the internal resonance, the large-amplitude roll motion occurred at wave amplitudes in the range 0.2–0.8 in (RMS), which is much smaller than those (1.0–4.0 in (RMS)) required to excite the roll motion in the absence of the internal resonance (see Oh *et al*. 1992). The two modes might be coupled nonlinearly; however, when there is no internal resonance to strengthen the nonlinear couplings, the energy fed into the heave mode is not transferred as easily to the roll mode.

It follows from the force–response curves that, as the wave amplitude is increased, the roll amplitude remains constant, decreases, and even dies out. Specifically, if the wave amplitude was increased continuously beyond the bifurcation value, the roll amplitude remained almost constant or even decreased instead of increasing mono-

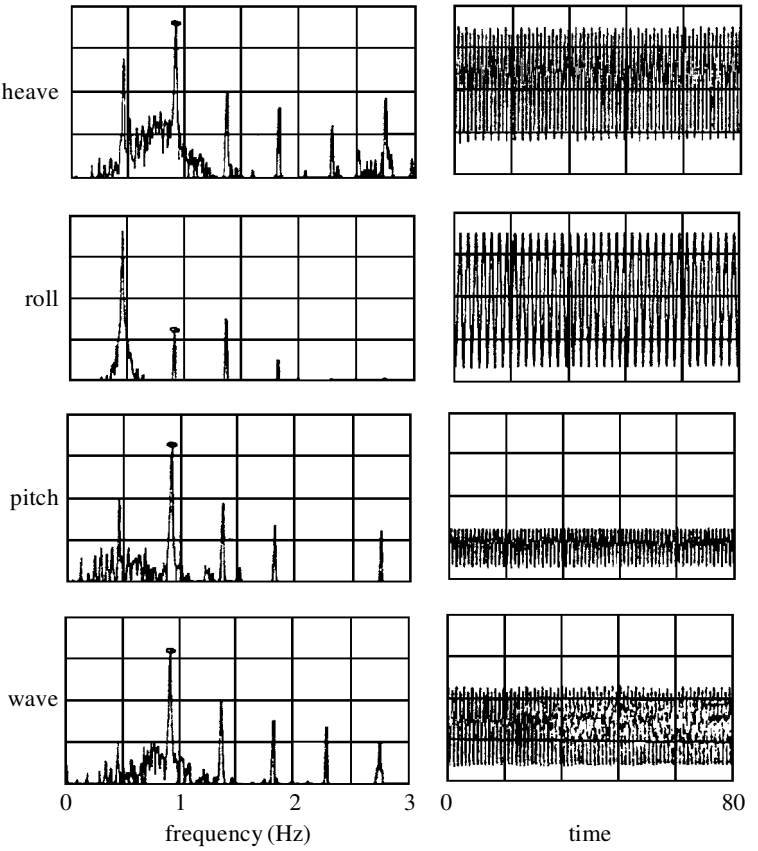

Figure 14. The spectra and time traces corresponding to point K in figure 11.

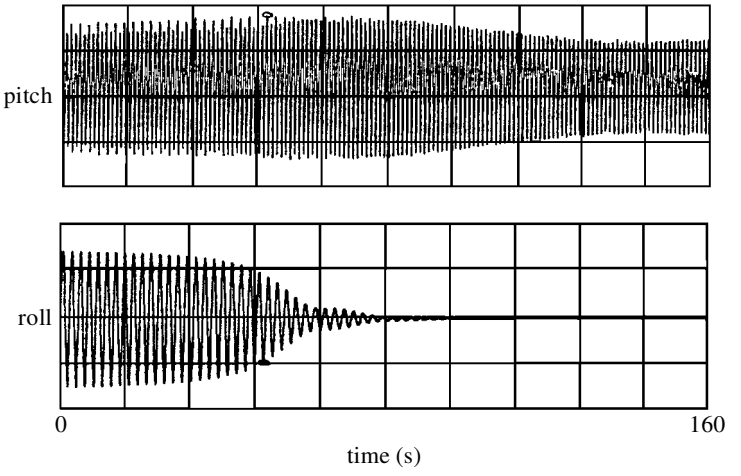

Figure 15. The time traces captured during the jump down.

tonically as predicted by the theoretical approach. This was also observed by other investigators (e.g. Dick *et al*. 1976). In the free-model scale experiments performed in the sea, they found that when the model was at zero speed in head waves, the roll amplitude was almost constant at higher wave heights, while the pitch amplitude increased linearly as the wave height increased.

The supercritical (or pitchfork) type of instability was not found. It is conjectured that higher-amplitude excitations are necessary.

4. Discrepancies between theory and experiment

We found good qualitative agreement between the theoretical and experimental results. However, there exist several discrepancies.

We note from force–response curves that as the wave amplitudes are increased, the magnitude of the large-amplitude roll motions decrease for all the cases considered here. This has also been observed by other investigators (see, for example, Dick *et al*. 1976). In the free-model scale experiment performed in the real sea, they showed that when the model was at zero speed in head seas the roll amplitude was almost constant at higher wave heights, while the pitch amplitude increased linearly as the wave heights increased.

The discrepancies may be due to one or more of the following four reasons. Firstly, the hydrostatic characteristics of a ship in waves can differ markedly from its characteristics in calm water. Secondly, while the roll motion causes relatively small waves that reflect from the sidewalls of the tank, the heave and pitch motions generate relatively large waves that also reflect from the sidewalls and form transverse standing waves on both sides of the model. The crests of these waves are a little aft of the midship section of the model, and they always meet the model just before the maximum roll angle occurs. Consequently, the reflected waves also act to limit the roll motion. Thirdly, because the model can pitch as well as heave, the difference in the phases of these two modes might cause the effective amplitude of the parametric excitation to decrease. It is a combination of the heave and pitch motions that produces the effective parametric excitation in the roll equation. Fourthly, it is worthwhile to consider the work of Eda *et al*. (1979) and Taggart & Kobayashi (1970). They showed that significant coupling of roll and yaw can develop due to the asymmetry of the underwater hull form of the heeled vessel. This is explained in the following way: the asymmetric form acts as a cambered low-aspect-ratio lifting body, which, together with the forward speed, produces sway forces and roll and yaw moments. When a vessel has relatively small values of GM, this can lead to dramatic increases in roll and yaw motions when the ship is operating in waves, a significant example of the nonlinear process in the responses of a vessel. Thus, in a test when yaw and sway motions are restricted, the reaction forces exerted on the vessel from the sides of the tank could decrease the roll motion.

The coupling between the pitch and yaw motions is another nonlinear effect that may need to be considered to understand the experimental results. It occurs when there is a drift angle between the vessel heading and the instantaneous velocity.

5. Summary

A theoretical and experimental study of the nonlinear dynamic characteristics and stability of floating vehicles has been presented. To investigate the complicated

responses of vehicles in regular waves, we modelled the vehicles by dissipative nonlinear dynamic systems subject to harmonic excitations. Two nonlinear mechanisms that cause large-amplitude motions were investigated. The first mechanism is internal or autoparametric resonance, the second is parametric resonance. They are exemplified by addressing the phenomenon of the indirect excitation of the roll motion of a vessel due to nonlinear couplings among its heave, pitch and roll modes.

The complicated responses due to nonlinear modal interactions were investigated analytically for a two-degree-of-freedom system modelling the pitch and roll motions of a vessel in the presence of a two-to-one internal resonance. These responses included periodic and periodically and chaotically modulated motions, coexistence of multiple motions, and jumps. Linear-plus-quadratic terms were used to model the roll damping, and a linear term was used to model the pitch damping. Also, the dynamic stability and large-amplitude motion of the roll mode due to an excitation of the pitch and heave modes (which excite the roll mode through parametric resonance) were studied. Because the physical models used in the present work are dissipative nonlinear dynamical systems subject to deterministic excitations, the results are applicable to many mechanical and structural systems.

Experiments were performed on models of actual vessels: a tanker and a destroyer. There were a number of previous experimental studies of the linear behaviour and impulsive loading (such as slamming) of vessels. However, very few experiments have been conducted to investigate the nonlinear couplings among the modes of motion and the resulting extraordinary responses, which cannot be explained by using the linear theory. The experiments demonstrated the jump phenomenon, the subcritical instability, and the coexistence of multiple motions, which are frequently observed in the response of many mechanical and structural systems. The experimental results are qualitatively in agreement with the results predicted by the theory.

This work was supported by the Office of Naval Research under grant no. N00014-96-1-1123.

References

Balachandran, B. & Nayfeh, A. H. 1991 Observations of modal interactions in resonantly forced beam-mass structures. *Nonlinear Dyn.* **2**, 77–117.

Bass, D. W. 1982 On the response of biased ships in large-amplitude waves. *Int. Shipbuilding Progr.* **29**, 2–9.

Blocki, W. 1980 Ship safety in connection with parametric resonance of the roll. *Int. Shipbuilding Progr.* **27**, 36–53.

Dick, D., Eng, C. & Corlett, E. C. B. 1976 The pan type post office cable repair ship. *Trans. R. Inst. Naval Architects* **119**, 305–322.

Eda, H., Falls, R. & Walden, D. A. 1979 Ship maneuvering safety studies. *Trans. Soc. Naval Architects Marine Engnrs* **87**, 229–250.

Feat, G. & Jones, D. 1984 Parametric excitation and the stability of a ship subjected to a steady heeling moment. *Int. Shipbuilding Progr.* **31**, 263–267.

Froude, W. 1863 Remarks on Mr Scott-Russell's paper on rolling. The papers of William Froude. *Trans. R. Inst. Naval Architects* **4**, 232–275.

Haddow, A. G., Mook, D. T. & Barr, A. D. S. 1984 Theoretical and experimental study of modal interaction in a two-degree-of-freedom structure. *J. Sound Vib.* **97**, 451–473.

Kerwin, J. E. 1955 Notes on rolling in longitudinal waves. *Int. Shipbuilding Progr.* **2**, 597–614.

Kinney, W. D. 1961 On the unstable rolling motions of ships resulting from nonlinear coupling with pitch including the effect of damping in roll. Institute of Engineering Research, University of California, Berkeley, Series no. 173, issue 3.

Lewis, E. V. (ed.) 1989 *Principles of naval architecture*, vol. III. New Jersey City, NJ: Society of Naval Architects and Marine Engineers.

Mook, D. T., Marshall, L. R. & Nayfeh, A. H. 1974 Subharmonic and superharmonic resonances in the pitch and roll modes of ship motions. *J. Hydronautics* **8**, 32–40.

Nayfeh, A. H. 1973 *Perturbation methods*. Wiley.

Nayfeh, A. H. 1981 *Introduction to perturbation techniques*. Wiley.

Nayfeh, A. H. 1988 On the undesirable roll characteristics of ships in regular seas. *J. Ship Res.* **32**, 92–100.

Nayfeh, A. H. & Mook, D. T. 1979 *Nonlinear oscillations*. Wiley.

Nayfeh, A. H. & Oh, I. G. 1995 Nonlinearly coupled pitch and roll motions in the presence of internal resonance. Part I. Theory. *Int. Shipbuilding Progr.* **42**, 295–324.

Nayfeh, A. H. & Sanchez, N. E. 1990 Stability and complicated rolling responses of ships in regular beam seas. *Int. Shipbuilding Progr.* **37**, 331–352.

Nayfeh, A. H. & Zavodney, L. D. 1988 Experimental observation of amplitude- and phase-modulated responses of two internally coupled oscillators to a harmonic excitation. *J. Appl. Mech.* **110**, 706–710.

Nayfeh, A. H., Mook, D. T. & Marshall, L. R. 1973 Nonlinear coupling of pitch and roll modes in ship motion. *J. Hydronautics* **7**, 145–152.

Nayfeh, A. H., Mook, D. T. & Marshall, L. R. 1974 Perturbation-energy approach for the development of the nonlinear equations of ship motion. *J. Hydronautics* **8**, 130–136.

Oh, I. G., Nayfeh, A. H. & Mook, D. T. 1992 Theoretical and experimental study of the nonlinearly coupled heave, pitch, and roll motions of a ship in longitudinal waves. In *Proc. 19th Symp. on Naval Hydrodynamics, Seoul, Korea, August 1992*.

Paulling, J. R. & Rosenberg, R. M. 1959 On unstable ship motions resulting from nonlinear coupling. *J. Ship Res.* **3**, 36–46.

Renilson, M. R. & Driscoll, A. 1982 Broaching—an investigation into the loss of directional control in severe following seas. *Trans. R. Inst. Naval Architects* **152**, 253–273.

Robb, A. M. 1952 *Theory of naval architecture*. London: Charles Griffin.

Sanchez, N. E. & Nayfeh, A. H. 1990 Nonlinear rolling motions of ships in longitudinal waves. *Int. Shipbuilding Progr.* **37**, 247–272.

Spyrou, K. J. 1996*a* Dynamic instability in quartering seas—the behavior of a ship during broaching. *J. Ship Res.* **40**, 46–59.

Spyrou, K. J. 1996*b* Dynamic instability in quartering seals. Part II. Analysis of ship roll and capsize for broaching. *J. Ship Res.* **40**, 326–336.

Spyrou, K. J. 1997 Dynamic instability in quartering seas. Part III. Nonlinear effects on periodic motions. *J. Ship Res.* **41**, 210–223.

Taggart, R. & Kobayashi, S. 1970 Anomalous behavior of merchant ship steering systems. *Marine Technol.* **7**, 205–215.